ELSEVIER

Journal of Structural Geology 26 (2004) 725–737

JOURNAL OF STRUCTURAL GEOLOGY

www.elsevier.com/locate/jsg

Rheology of plasticine used as rock analogue: the impact of temperature, composition and strain

Janet Zulauf*, Gernold Zulauf

Department of Geology and Mineralogy, University of Erlangen-Nuremberg, Schlossgarten 5, Erlangen 91054, Germany

Received 18 September 2002; received in revised form 4 July 2003; accepted 4 July 2003

Abstract

Uniaxial compression tests have been carried out to determine the temperature-dependent rheology of plasticine commonly used for tectonic modelling. The original plasticine types (*Kolb brown*, *Beck's orange*, *Beck's green*, *Weible special soft*) are characterized by strain-rate softening with power law exponents (n) and apparent viscosities (η) ranging from 5.8 to 7.3 and 3.4×10^5 to 2.2×10^7 Pa s, respectively (if $e = 10\%$, $\dot{E} = 4 \times 10^{-3}$ s^{-1}, and $T = 25$ °C). *Beck's orange* shows steady-state creep, whereas the other types show strain hardening. The activation energy, determined for 20 °C $\leq T \leq$ 35 °C, is ranging from 323 $\pm$ 34 to 488 $\pm$ 22 kJ mol^{-1}. A rise in temperature results in linear decreases of n and η and a reduction in the degree of strain hardening. Steady-state creep and major changes in n and η have further been observed at decreasing filler-matrix ratios, the latter being obtained by adding oil to the original plasticine. The new results suggest that plasticine can be used to model the deformation of natural rocks undergoing dislocation creep. Various rock analogues with strain hardening or steady-state creep, and prescribed stress exponents ranging from 3.4 to 12.3, can be easily produced by changing the temperature and/or the filler-matrix ratio of commercial plasticine types.

Keywords: Plasticine; Rheology; Analogue modelling; Power-law creep; Strain hardening

1. Introduction

Our knowledge on rock deformation arises from field studies and laboratory experiments, the latter being applied either to natural rocks or to weaker analogue material. Experimental deformation of natural rocks results in constitutive flow laws, the extrapolation of which suggests the continental crust to be rheologically stratified (e.g. Brace and Kohlstedt, 1980; Chen and Molnar, 1983; Ranalli and Murphy, 1987; Murphy, 1989; Ranalli, 1995). Coulomb brittle rheologies are characteristic for shallow crustal levels, whereas thermally activated viscous creep is dominant at depth. Given that recrystallization-accommodated dislocation creep is active at deeper structural levels, where temperatures are higher than about half the absolute melting temperature (Poirier, 1985, p. 111, and references therein), the strain rate ($\dot{E}$) is related to the applied differential stress (σ) by a power law.

The power factor or stress exponent (n) varies for rocks between 1 and 10 (Weijermars, 1986), but values between 2 and 5 predominate in coarse-grained rocks (e.g. Kirby, 1983; Kronenberg and Tullis, 1984; Carter and Tsenn, 1987; Gleason and Tullis, 1995; Ranalli, 1995; Talbot, 1999). In cases of low differential stress and small grain size, viscous creep may further be accommodated by solution and precipitation or by volume or grain-boundary diffusion, all of which are based on a linear (Newtonian) relation between stress and strain rate.

To simulate viscous deformation of lower crustal rocks under laboratory conditions, various types of analogue material, such as wax, polymers (e.g. polydimethylsiloxane, PDMS), polymers with fillers (e.g. silicone or bouncing putty), plasticine, or combinations of these materials have been used in the past. Some of these materials show linear (Gum rosin) and others show non-linear (e.g. plasticine, wax) viscous behaviour.

Plasticine has been used to simulate geological structures such as folds, boudins, diapirs etc. (Ramberg, 1955; Watkinson, 1975; Peltzer et al., 1984; Sokoutis, 1987; Gosh et al., 1995; Kobberger and Zulauf, 1995; Kidan and

* Corresponding author. Tel.: +49-9131-85-22617; fax: +49-9131-85-29295.

E-mail address: janet@geol.uni-erlangen.de (J. Zulauf).

0191-8141/$ - see front matter © 2003 Elsevier Ltd. All rights reserved.
doi:10.1016/j.jsg.2003.07.005

Cosgrove, 1996; Acocella and Mulugeta, 2002; Zulauf et al., 2003). According to previous studies, carried out largely at room temperature, plasticine can be regarded as a non-linear, strain-rate softening, but strain hardening material consisting of a weak organic matrix and mineral fillers (McClay, 1976; Peltzer et al., 1984; Weijermars, 1986; Kobberger and Zulauf, 1995; Schöpfer and Zulauf, 2002). As the flow curves and stress exponents of plasticine and common natural rocks are similar, plasticine can be applied to simulate the deformation of rocks undergoing dislocation creep. However, because of strain hardening, plasticine does not reach a steady state during viscous deformation. Moreover, as the impact of the temperature on the rheology of plasticine is largely unknown, plasticine cannot be used to simulate deformation in settings where temperature-induced variations in mechanical properties of rocks must be taken into account (e.g. Cobbold and Jackson, 1992; Rossetti et al., 2001; Wosnitza et al., 2001). In contrast to plasticine, the temperature-dependent rheology is well known for other rock analogues such as paraffin wax (Mancktelow, 1988; Rossetti et al., 1999), bouncing putties (Weijermars, 1986; Hailemariam and Mulugeta, 1998) and PDMS (Weijermars, 1986).

The present paper presents new data on the composition and rheology of different kinds of commercially available plasticine and plasticine–oil mixtures, which show both strain hardening and steady-state creep. Values for the activation energy will be presented for the first time. It will be shown how finite strain, temperature, amount of added oil, and type of fillers influence the rheology of plasticine. We further emphasize that care is needed when preparing plasticine samples. The new results should be of interest for all workers whose models are based on rheologically stratified analogue material and temperature-induced variations in rheology.

2. Sampling material

We investigated the following types of commercially available plasticine produced by German manufacturers: (1) Beck's green and (2) Beck's orange made by Beck's Plastilin, Gomaringen, Germany, (3) Kolb brown made by Kolb, Hengersberg, Germany, and (4) Weible special soft made by Weible KG, Schorndorf, Germany. The plasticine types Beck's orange and Kolb brown were mixed with liquid paraffin produced by DEA Mineralöl AG, Hamburg, Germany, to change viscosity and stress exponent.

3. Methods

3.1. Rheological tests

More than 380 uniaxial compression tests were performed using the testing apparatus ZWICK/Z050 at the Lehrstuhl für Polymerwerkstoffe, Universität Erlangen-Nürnberg. The computer aided machine worked at constant velocity ranging from 400 to less than 0.04 mm s^{-1}. The plate distance (dl) and the force (F) were recorded at steps of 0.02 to 1 s. As the initial samples were cubes or cylinders, respectively, the stress (σ) was calculated using the following equations:

$$\sigma = \frac{F(l - dl)}{l^3} \quad (1)$$

$$\sigma = \frac{F(l - dl)}{\pi r^2 l} \quad (2)$$

where l is the edge length of the cube and the height of the undeformed cylinder, respectively, and r is the radius of the cylinder (Fig. 1a).

The finite longitudinal strain rate is calculated by equation:

$$\dot{E} = \frac{e(t)}{dt} \quad (3)$$

where e is the finite strain and t is the time.

As the ram speed is constant throughout a test, the strain rate is not constant. However, at $e \leq 50\%$ the difference between finite and incremental strain rate is small and can be neglected.

We tested original types of Beck's orange, Beck's green and Kolb brown plasticine at 20, 25, 30 and 35 °C. The uncertainty in temperature is ±1 °C. To increase the temperature of a 6 × 6 × 6 cm block at 5 °C, a period of ca. 1 h is required. This holds for measurements between 20 and 50 °C. At ca. 70–80 °C plasticine starts to flow due to gravitational forces. Further we analysed Weible special soft and 11 plasticine/oil mixtures at 25 °C. The samples

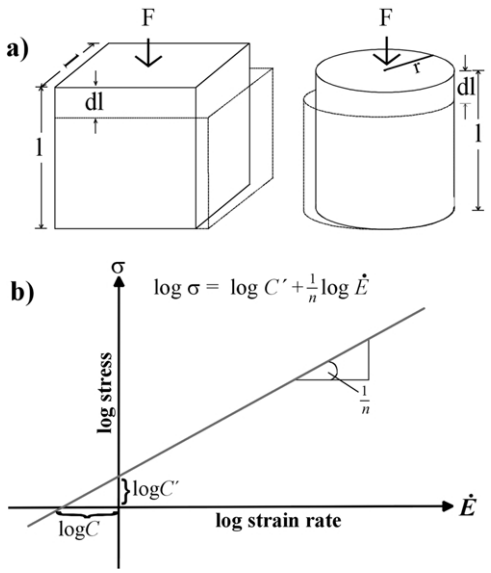

Fig. 1. (a) Cartoon showing undeformed and deformed sample; F = force; l = length of undeformed sample; dl = shortening increment. (b) Schematic diagram of log differential stress (σ) vs. log strain rate ($\dot{E}$). Slope of regression line gives $1/n$; for further explanation see text.

were $4.5 \times 4.5 \times 4.5$ cm blocks for the hard plasticine, $6 \times 6 \times 6$ cm blocks for the normal plasticine, and cylinder blocks with a diameter and height of 10 cm for the special soft plasticine. To reduce friction, the piston of the machine and the surfaces of the samples were lubricated with Vaseline. Plasticine is an approximately incompressible fluid. Thus homogeneous constant-volume deformation can be assumed.

Rheological calibration was performed with a series of strain rates (7.6×10^{-2}–$5.5 \times 10^{-5}\ s^{-1}$) applied to the cubes or cylinder blocks and measuring the change of the differential stress as the axial strain progresses up to 15 or 20%. Three plasticine types were deformed up to 50% strain.

Stress relaxation tests were carried out using similar strain rates as described above. The stress relaxation was recorded for 5 min after 1, 5, 10, 15 and 20% axial strain was achieved.

To mould the plasticine into cubes, the viscosity of the hard types was decreased by increasing its temperature up to ca. 50 °C for a maximum of 1 h. Caution is needed when moulding the samples. The viscosity of the heated samples is significantly controlled by the degree of kneading during the cooling period. Samples that are heated to $T = 55$ °C and cool down to room temperature without deformation are much harder than those samples that are moulded by hand during cooling (see below). Further caution is needed to avoid air bubbles, which might be introduced into the plasticine during the moulding process. These bubbles are possible sites where shear fractures may occur.

3.2. Calculation of material parameters

At constant temperatures the constitutive flow law of plasticine can be written as:

$$\dot{E} = C\sigma^n \tag{4}$$

where $\dot{E}$ is the longitudinal strain rate, C the material constant, n the stress exponent and σ the differential stress (McClay, 1976).

The apparent dynamic viscosity (η), the material constant (C) and the stress exponent (n) were calculated for 10% strain. The slope of a linear best-fit least-squares regression of a log strain-rate vs. log stress diagram yields the stress exponent. The intercept at the ordinate yields the material constant (C). It is important to note that the major uncertainty concerns the stress, whereas the strain rate is largely independent, apart from the uncertainties of the machine, the latter being negligible. Therefore we use a log stress vs. log strain-rate plot, where the slope of the regression line yields $1/n$, and C' is the intercept along the vertical stress axis (Fig. 1b).

Starting from Eq. (4), the material constant can be calculated by substituting ($\sigma/\dot{E}$) couples determined experimentally (Weijermars and Schmeling, 1986). We calculated the material constant using the linear best-fit least-squares regression (Fig. 1b) and the following equation:

$$C = 10^{-\log C' n} \tag{5}$$

The viscosity can be calculated by the following equation:

$$\eta = \frac{\sigma}{2\dot{E}} \tag{6}$$

Combining Eqs. (4) and (6) yields Eq. (7), which can be used to calculate the viscosity using all data couples:

$$\eta = \frac{1}{2C^{\frac{1}{n}}} \dot{E}^{\frac{1}{n}-1} \tag{7}$$

The relation between temperature and viscosity is described by the activation energy (Q) of the constitutive flow law

$$\dot{E} = A\sigma^n \exp(-Q/\mathrm{RT}) \tag{8}$$

where A is a constant, R is the Boltzmann's gas constant and T is the absolute temperature (Weertman, 1968).

The activation energy was derived using Arrhenius plots, where ln strain rate is plotted vs. the inverse temperature. From a linear regression of this plot the average activation energy can be calculated (e.g. Hailemariam and Mulugeta, 1998). The slope of the regression line is $-Q/\mathrm{R}$. The strain rate ($\dot{E}$) for particular stresses was determined using log stress vs. log strain-rate diagrams as shown in Fig. 1b.

3.3. Analyses of fillers

To separate possible inorganic fillers from the organic plasticine matrix, the latter was dissolved using carbon tetrachloride. The residues were investigated using SEM and X-ray diffraction analyses.

4. Results

4.1. Composition of plasticine

The exact composition of the investigated plasticine is confidential. According to some details of the producers, the organic matrix of plasticine consists of wax, Vaseline, oil and lubrication solvent. The fillers are generally inorganic, but in the case of Beck's orange plasticine they consist of potato starch. Fillers of Beck's green largely consist of calcite. Kolb brown includes barite, kaolinite and minor amounts of fluorite and illite. Weible special soft consists of calcite and minor amounts of kaolinite. Some of the plasticine types include small amounts of dyes such as titanium dioxide, magnetite or haematite. The calcite and

barite fillers of Beck's green and Kolb brown are plate shaped.

The amount of filler volume of the original plasticine types investigated ranges from 56% (Beck's orange) to 40% (Weible special soft). To calculate the amount of filler for Beck's orange, we used the density of corn starch (1.48 g cm^{-1}; Müller, 1998). The density ranges from 1.99 g cm^{-1} for Kolb brown to 1.13 g cm^{-1} for Beck's orange plasticine (Table 1).

4.2. Rheology of plasticine types at $T = 25$ °C

Results of constant strain-rate tests of the original plasticine types, carried out at $T = 25$ °C, are presented in form of stress vs. strain plots (Figs. 2 and 3). The plots show non-linear flow curves with an initial linear increase of stress and strain until plastic yielding is achieved at $e < 2.5\%$. Only Beck's orange plasticine shows steady-state flow at $e > 5\%$ (Fig. 2). The other plasticine types are characterized by strain hardening. It is obvious from the stress vs. strain plots that multiple measurements at one and the same strain rate do not yield the same curves. However, the strain vs. stress curves, determined at one particular strain rate, are usually different from those obtained by using other strain rates. The stress exponent and apparent dynamic viscosity, determined at 10% strain and a strain rate of 4×10^{-3} s^{-1}, are listed in Table 1. Log stress vs. log strain-rate plots and resulting stress exponents are shown in Fig. 4. The fit of the regression lines is usually very good as shown by coefficients of correlation (R_k) larger than 0.9 and large amounts of data points (N).

At 10% strain, $T = 25$ °C and a strain rate of 4×10^{-3} s^{-1}, the apparent viscosity of the original plasticine types varies by two orders of magnitude. The weakest plasticine is Weible special soft, which yields a viscosity of $\eta = 3.4 \times 10^5$ Pa s. The hardest plasticine is Kolb brown with $\eta = 2.2 \times 10^7$ Pa s. The n-values are ranging from 5.8 (Kolb brown) to 7.3 (Weible special soft) suggesting strain-rate softening behaviour.

The behaviour of Beck's orange, Beck's green and Kolb brown plasticine has further been tested for high strains up to 50%. The stress vs. strain plots indicate that for Beck's green and Kolb brown the degree in strain hardening does not significantly change at high strains (Fig. 5). Beck's orange shows still steady-state creep.

To quantify the amount of strain hardening at $T = 25$ °C, the viscosity of the original plasticine types has been calculated at different finite strains, the latter increasing at 1% steps. Beck's orange plasticine shows an almost constant viscosity at $e > 7\%$ suggesting steady-state flow (Fig. 6a). This is in good agreement with the shape of the strain vs. stress curves (Fig. 2a). Steady-state flow at

Table 1
Density and rheological data of investigated plasticine types and plasticine/oil mixtures. Parameters calculated at a strain rate $\dot{E} = 4 \times 10^{-3}$ s^{-1}, $T = 25$ °C and a strain of $e = 10\%$

	Temperature [°C]	Density (ρ) [g cm^{-3}]	Added oil [ml kg^{-1}]	Viscosity (η) [Pa s]	Stress exponent (n)	Material constant (C) [MPa^{-n} s^{-1}]
Kolb brown	20	–	–	2.56×10^7	6.9	2.19×10^2
	25	*1.99*	–	*2.23×10^7*	*5.8*	*9.40×10^1*
	30	–	–	1.74×10^7	4.9	6.84×10^1
	35	–	–	1.01×10^7	4.7	5.26×10^2
	25	1.85	25	1.43×10^7	6.5	5.06×10^3
	25	1.74	50	9.40×10^6	7.0	6.26×10^5
	25	1.75	75	4.91×10^6	8.8	9.98×10^9
	25	1.75	100	4.04×10^6	8.8	5.56×10^{10}
	25	1.71	125	3.03×10^6	10.2	1.11×10^{14}
	25	1.63	150	2.05×10^6	11.7	2.85×10^{18}
Beck's green	20	–	–	1.43×10^7	10.0	1.02×10^7
	25	*1.72*	–	*1.13×10^7*	*7.4*	*2.26×10^5*
	30	–	–	7.25×10^6	6.2	1.85×10^5
	35	–	–	4.46×10^6	5.0	7.35×10^4
	25[a]	–	25	7.01×10^6	10.9	1.95×10^{11}
	25[a]	1.63	50	4.85×10^6	10.4	1.67×10^{12}
Beck's orange	20	–	–	8.10×10^6	7.8	9.33×10^6
	25	*1.13*	–	*7.85×10^6*	*6.9*	*8.56×10^5*
	30	–	–	5.25×10^6	5.9	5.70×10^5
	35	–	–	3.15×10^6	4.7	1.31×10^5
	25	1.12	25	6.16×10^6	12.3	4.27×10^{13}
	25	1.10	50	2.72×10^6	10.3	5.45×10^{14}
	25	1.12	75	2.29×10^6	9.1	2.11×10^{13}
	25	1.12	100	2.06×10^6	7.2	2.23×10^{10}
	25	1.07	125	1.66×10^6	7.0	4.57×10^{10}
Weible white	*25*	*1.56*	–	*3.40×10^5*	*7.3*	*2.12×10^{16}*

[a] Basic data taken from Schöpfer (2000).

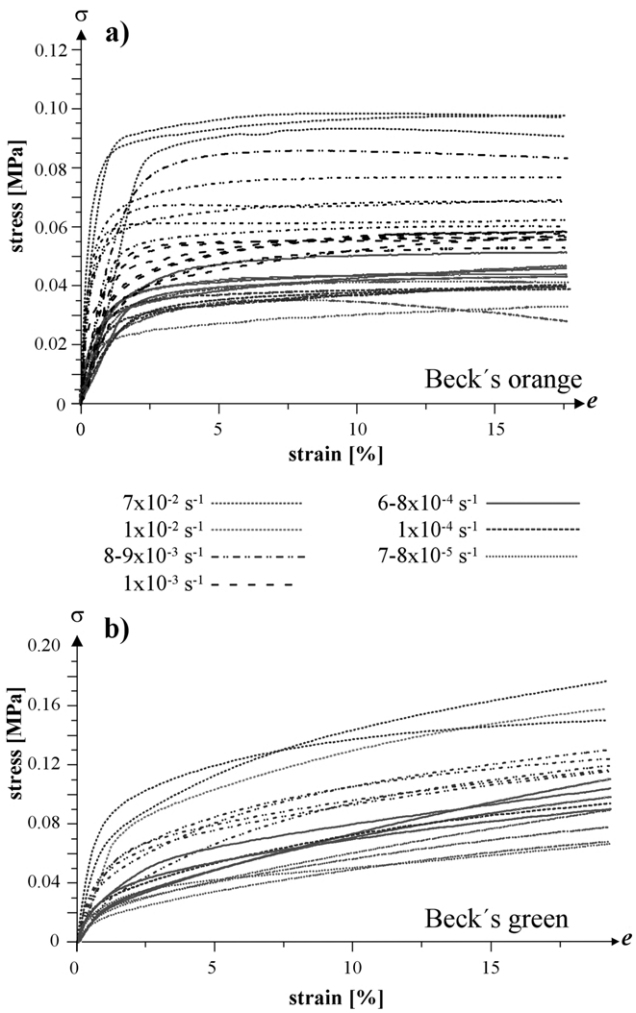

Fig. 2. Stress vs. strain plots at $T = 25$ °C for (a) Beck's orange plasticine, $N = 27$ and (b) Beck's green plasticine, $N = 17$; N = number of runs.

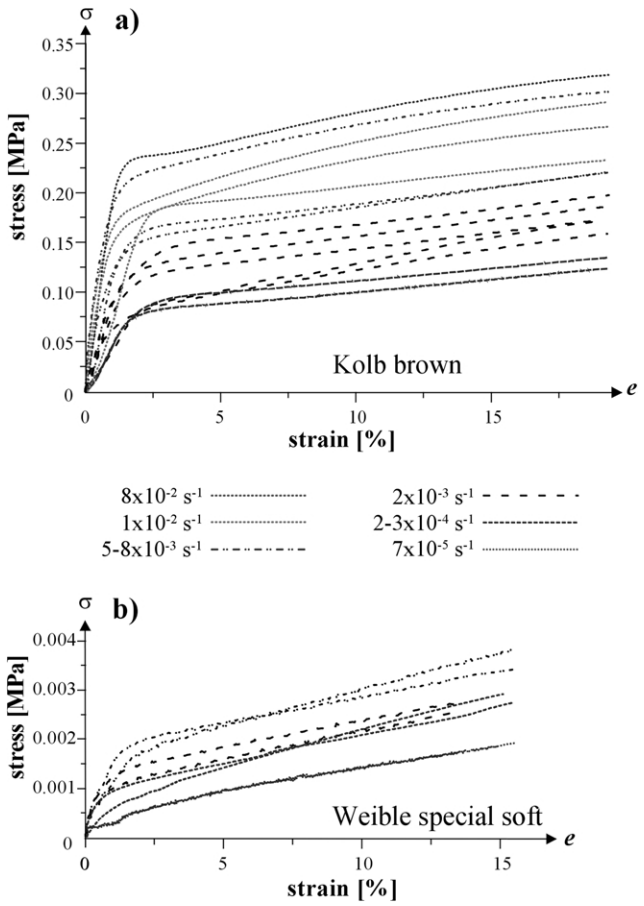

Fig. 3. Stress vs. strain plots at $T = 25$ °C for (a) Kolb brown plasticine, $N = 14$ and (b) Weible special soft plasticine, $N = 7$; N = number of runs.

$e > 10\%$ is consistent with an almost constant stress exponent at ca. 7 (Fig. 6b). The other plasticine types show strain hardening. If for Kolb brown plasticine the yield point is passed at ca. 4% strain, a rise in strain magnitude of about 5% implies an increase in viscosity from 2.25×10^7 to 2.50×10^7 Pa s. The degree in strain hardening is still less significant for Beck's green plasticine (Fig. 6a). Strain hardening affects also the stress exponent and this is particularly evident for Beck's green plasticine (Fig. 6b).

The material constant (C) also changes with increasing strain. A linear relation characterizes Beck's orange plasticine (Fig. 7). If strain increases from 2 to 16%, the material constant increases by one order of magnitude. Beck's green and Kolb brown, on the other hand, are characterized by a non-linear relation between strain and material constant. In the case of Beck's green, the constant decreases until 6% strain is achieved. At higher strains it increases (Fig. 7). Kolb brown shows the opposite behaviour.

The results of stress relaxation tests for Kolb brown, Beck's green and Beck's orange are shown in stress vs. time plots (Fig. 8). At high strain rates (1×10^{-2}–1×10^{-3} s^{-1}) the relaxation curves show an initial very strong increase in stress (elastic part), without reaching plastic yielding, and is followed by a sudden decrease in stress and a transition to slow decrease resting in steady state. At the slow strain rate (1×10^{-4} s^{-1}) relaxation starts after yielding.

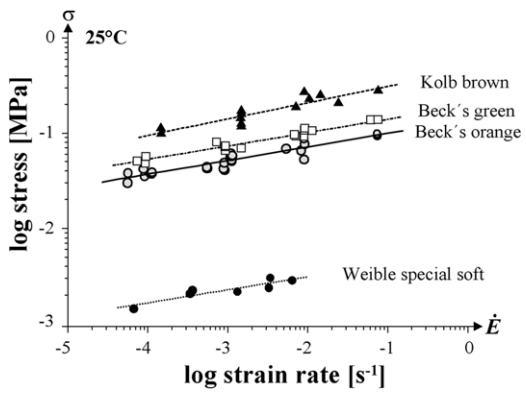

Fig. 4. Log stress vs. log strain rate plot for original plasticine types at 10% axial strain and $T = 25$ °C. Kolb brown $R_k = 0.92$, $N = 14$; Beck's green $R_k = 0.98$, $N = 17$; Beck's orange $R_k = 0.95$, $N = 27$, and Weible special soft $R_k = 0.91$, $N = 7$. Best-fit regression lines are also shown. R_k = regression coefficient, N = number of data points.

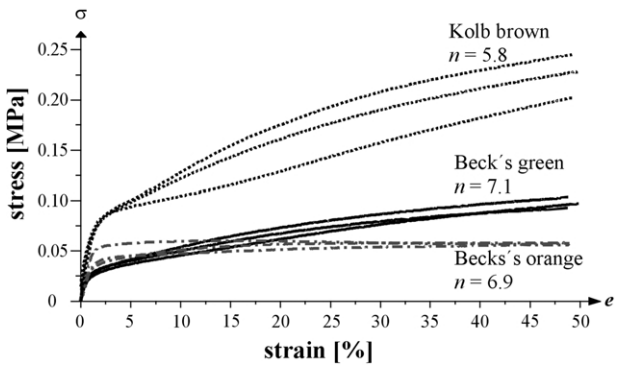

Fig. 5. Stress vs. strain plot for Kolb brown, Beck's green and Beck's orange plasticine including high finite strains up to 50% at $\dot{E} = 1.3 \times 10^{-3}\ s^{-1}$ and $T = 25$ °C.

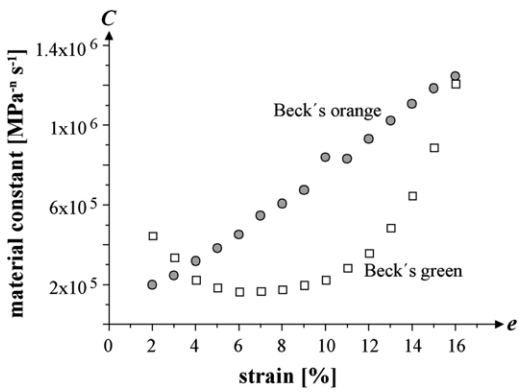

Fig. 7. Plots showing material constant vs. strain for Beck's green, Beck's orange plasticine at $T = 25$ °C and $\dot{E} = 4 \times 10^{-3}\ s^{-1}$.

4.3. Influence of temperature

There is a significant change in viscosity and stress exponent with temperature. Examples of flow curves are shown for heated Kolb brown plasticine (Fig. 9a–c). A rise in temperature results in lower stresses for plastic yielding and flattening of the slope of the curves when deformation occurs in the plastic (viscous) regime. These phenomena imply a drop in apparent viscosity and reduction in the degree of strain hardening. The impact of temperature on the stress exponent for Kolb brown plasticine is shown in log stress vs. log strain rate plot (Fig. 9d). The other plasticine types show similar behaviour (Table 1).

If the temperature rises at 5° steps from 20 to 35 °C, both the viscosity and the stress exponent are changing almost linearly (Fig. 10a and b). A rise in temperature from 20 to 35 °C causes a drop in viscosity up to 1/4–1/2 order of magnitude (Table 1; Fig. 10a). A temperature-dependent change of the stress exponent is most significant for Beck's green where a rise in temperature from 20 to 35 °C leads to a drop in the stress exponent from 10 to 5 (Fig. 10b). The material constant (C) changes unsystematically by one order of magnitude at maximum (Table 1). The degree in strain hardening is reduced at higher temperatures.

The activation energy has been determined for the original plasticine types Beck's orange, Beck's green, and Kolb brown using Arrhenius diagrams (Fig. 11). Beck's orange yields the lowest activation energy at 323 ± 34 kJ mol^{-1} (Fig. 11a), whereas Beck's green yields the highest value at 488 ± 22 kJ mol^{-1} (Fig. 11b). Kolb brown is situated in between at 411 ± 24 kJ mol^{-1} (Fig. 11c).

4.4. Influence of matrix/filler ratio

Adding oil to Kolb brown, Beck's green and Beck's orange plasticine results in a change of apparent viscosity and stress exponent. The amount of added oil was increased step by step with one step including 25 ml kg^{-1}. The maximum amount of added oil was set at 150 ml kg^{-1}. Examples of flow curves of plasticine/oil mixtures are shown for Kolb brown (Fig. 12a and b). Added oil results in decreasing stresses at the yield point. The higher the amount of added oil, the higher the reduction in strain hardening, approximating steady-state flow. The change in the n-value of Kolb brown is shown by the different regression lines in the log stress vs. log strain-rate diagram (Fig. 12c). The stress exponent increases almost linearly with added oil from 5.8 to 11.7 (Fig. 13a). The stress exponent of modified Beck's orange plasticine shows a peculiar behaviour. Only

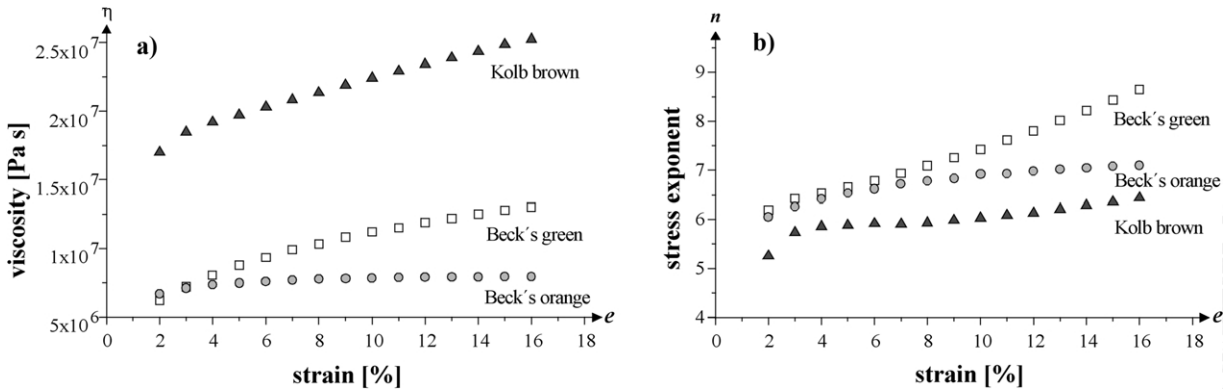

Fig. 6. Plots showing (a) apparent viscosity vs. strain and (b) stress exponent vs. strain for Kolb brown, Beck's green and Beck's orange plasticine at $T = 25$ °C and $\dot{E} = 4 \times 10^{-3}\ s^{-1}$.

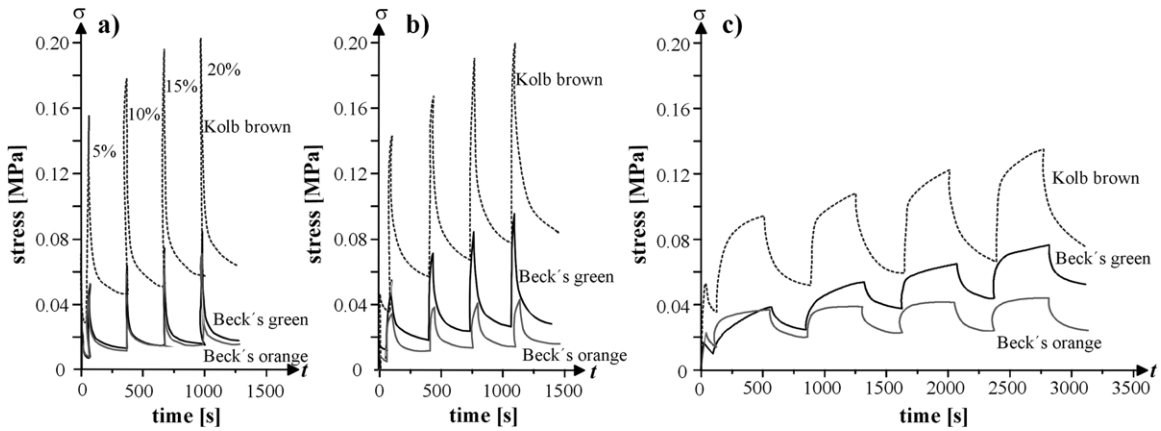

Fig. 8. Relaxation curves for Kolb brown, Beck's green and Beck's orange plasticine at different strain rates (a) $\dot{E} = 1.1 \times 10^{-2}\ s^{-1}$, (b) $1.1 \times 10^{-3}\ s^{-1}$, (c) $1.1 \times 10^{-4}\ s^{-1}$ and $T = 25$ °C; 1, 5, 10, 15 and 20% strain values are indicated.

small amounts of oil (25 ml kg^{-1}) result in a striking increase of the stress exponent from 6.9 to 12.3. Further addition of oil reduces the stress exponent. The original *n*-value is reached again if 100 or 125 ml oil are added to 1 kg plasticine (Fig. 13a). There is a non-linear relation between the amount of added oil and the apparent viscosity for all of the plasticine types considered (Fig. 13b). Adding 150 ml oil to 1 kg of Kolb brown plasticine causes a drop in apparent viscosity by about one order of magnitude. For Beck's orange and Beck's green plasticine this oil-related drop in viscosity is less significant.

Adding oil to plasticine also causes a change in the material constant (*C*), which is most significant for Kolb brown plasticine. Adding 150 ml oil to 1 kg plasticine increases the *C*-value by 15 orders of magnitude (Table 1).

4.5. Repeatability and uncertainties of the results

To show the repeatability of our rheological data, the same supply of Beck's green plasticine has been tested twice, but independently. One set of rheological data is shown in the present study, the other set is a recalculated database. Further we measured a new supply. The different data are listed in Table 2. There is only a weak difference in

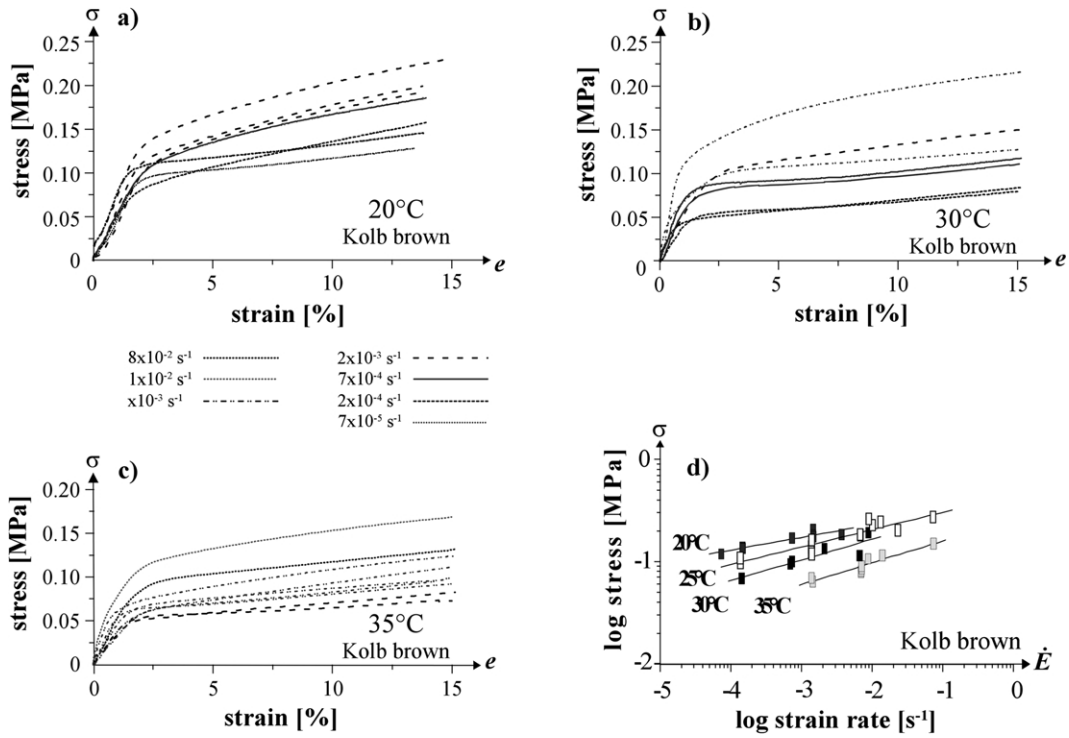

Fig. 9. Stress vs. strain plots for Kolb brown plasticine at (a) 20 °C, (b) 30 °C, and (c) 35 °C; (d) log stress vs. log strain rate plot for Kolb brown plasticine at 10% strain and $T = 20$ °C, $R_k = 0.93$, $N = 7$; $T = 25$ °C, $R_k = 0.92$, $N = 14$; $T = 30$ °C, $R_k = 0.92$, $N = 7$; and $T = 35$ °C, $R_k = 0.94$, $N = 9$. Best-fit regression lines are shown. R_k = regression coefficient, N = number of data points.

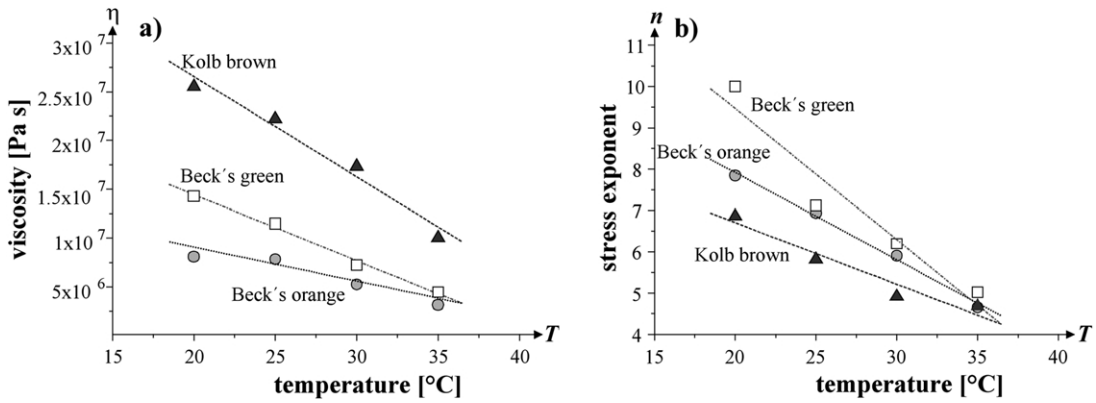

Fig. 10. Plots showing (a) viscosity vs. temperature for the plasticine types Beck's orange, $R_k = 0.961$; Beck's green, $R_k = 0.996$; and Kolb brown, $R_k = 0.985$. (b) Stress exponent vs. temperature for the plasticine types Beck's orange, $R_k = 0.998$; Beck's green, $R_k = 0.96$; and Kolb brown, $R_k = 0.97$; R_k = regression coefficient.

Table 2
Material parameters for Beck's green plasticine, derived from two independent measurements (this study and a database of the old supply) and a new supply; parameters calculated at 10% strain, for $\dot{E} = 4 \times 10^{-3}\ s^{-1}$ and $T = 25\ °C$

	Viscosity (η) [Pa s]	Stress exponent (n)	Material constant (C) [MPa^{-n} s^{-1}]
This study	1.13×10^7	7.4	2.26×10^5
Old supply[a]	1.10×10^7	6.5	2.94×10^4
New supply	1.11×10^7	8.6	1.22×10^5

[a] From Schöpfer (2000).

the apparent viscosity. The difference in n-value of one and the same material suggests the uncertainty of n to be about 0.6. The higher n-value of the new supply might result from a difference in composition.

Apart from strain hardening, there is another possibility to make plasticine mechanically stronger. Warming up plasticine to a temperature of ca. 55 °C and cooling down to room temperature without deformation results in significant hardening. 'Warming–cooling hardening' will disappear after weak, but pervasive deformation. Hardening will also be reduced if plasticine is deformed *during* cooling. The hardening effect is still more pronounced at higher temperatures. To quantify the amount of 'warming–cooling hardening', we tested samples that were heated to 55 °C and subsequently cooled to 25 °C without deformation. In Fig. 14 the stress–strain curve is shown for heated and cooled Kolb brown (curve 1). In a second run, a shear fracture in the cooled sample led to transient strain softening (curve 2 in Fig. 14), which occurs at high strain rates ($> 10^{-2}\ s^{-1}$ and $10^{-3}\ s^{-1}$ for hard/cooled samples).

We further tested samples that were pre-strained ($\cong 4\%$) and samples that were equipped with air bubbles. Closing of pre-existing inclusions of air bubbles caused a significant reduction in viscosity and a delay in the stress increase (curve 4 in Fig. 14). A pre-existing strain led to an increase in viscosity and absence of a concise yield point (curve 3 in Fig. 14). A normal run is shown by the shaded area (labelled 5 in Fig. 14).

5. Discussion

5.1. Influence of filler, temperature and strain on the rheology of plasticine

The results presented above suggest that all types of commercial plasticine considered in the present study are strain-rate softening materials with a poorly defined yield transition from elastic to plastic behaviour at axial strains ranging from ca. 1 to ca. 3%. The stress–strain curves at

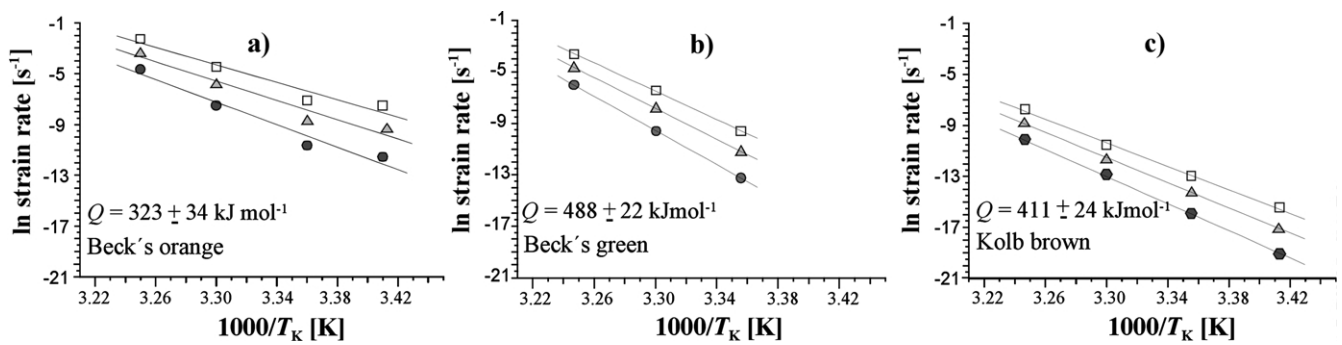

Fig. 11. Arrhenius diagrams for (a) Beck's orange (b) Beck's green and (c) Kolb brown plasticine. Squares, triangles and circles indicate data derived from stresses at 0.05, 0.04, and 0.03 MPa, respectively. The temperature range is 20–35 °C.

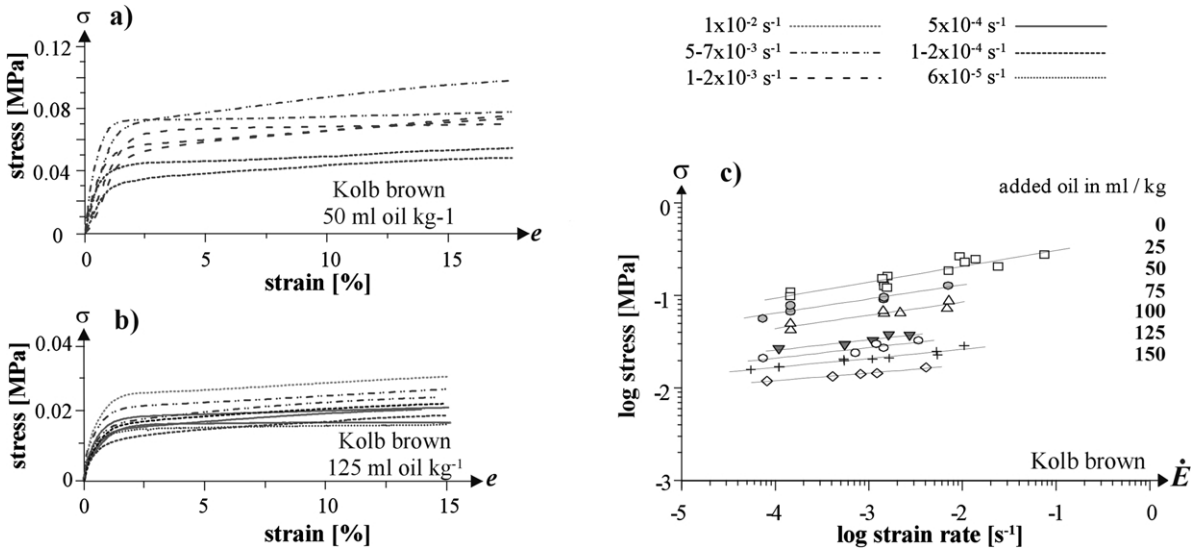

Fig. 12. Stress vs. strain plots for Kolb brown plasticine modified by different amounts of added oil at $T = 25$ °C for (a) 50 ml oil kg^{-1} and (b) 125 ml oil kg^{-1}. (c) Log stress vs. log strain rate plot for Kolb brown plasticine at 10% strain, $T = 25$ °C and different amounts of added oil: 0 ml kg^{-1}, $R_k = 0.92$, $N = 14$; 25 ml kg^{-1}, $R_k = 0.97$, $N = 6$; 50 ml kg^{-1}, $R_k = 0.96$, $N = 7$; 75 ml/kg, $R_k = 0.95$, $N = 5$; 100 ml kg^{-1}, $R_k = 0.92$, $N = 5$; 125 ml kg^{-1}, $R_k = 0.98$, $N = 10$; 150 ml kg^{-1}, $R_k = 0.99$, $N = 5$; best-fit lines are also shown; R_k = regression coefficient, N = number of data points.

25 °C indicate that the flow behaviour of plasticine approaches that of the elastic–plastic model for a continuum. At a temperature of 25 °C the stress exponent of the original plasticine types is similar, ranging from 5.8 to 7.4, whereas the apparent viscosity differs by two orders of magnitude (3.4×10^5–2.2×10^7 Pa s, for $e = 10\%$ and $\dot{E} = 4 \times 10^{-3}$ s^{-1}). Similar results have been obtained in previous rheological studies. McClay (1976) stated that Harbuts Plasticine behaves like a Reiner–Rivlin fluid with stress exponents varying between 7.5 and 9.4 and a viscosity range of 8.9×10^7–1.7×10^9 Pa s (at $e = 10\%$, $\dot{E} = 1.0 \times 10^{-3}$ s^{-1} and $T = 25$ °C). For Weible red and Weible white plasticine, the latter mixed with oil, Kobberger and Zulauf (1995) determined stress exponents of 7.2 and 3.4 and viscosities at 2.2×10^6 and 2.3×10^5 Pa s, respectively (at $e = 5\%$, $\dot{E} = 8 \times 10^{-3}$ s^{-1} and $T = 20$ °C). For white Plastilina from Beckers Dekorina, Sweden, a viscosity of ca. 1×10^5 Pa s, and a stress exponent of 9.5 has been determined (at $\dot{E} \approx 1$ s^{-1} and $T = 24$ °C, Weijermars, 1986).

Three of the original plasticine types investigated show strain hardening, the degree of which did not significantly change during deformation even at higher strains. This observation is not in line with observations made by McClay (1976), who explained sudden increases in strain hardening of Harbuts Plasticine at higher strains by the development of microshears. Strain hardening of various types of plasticine has been described further by Sofuoglu and Rasty (2000).

However, strain hardening is not inherent to every plasticine type. According to our knowledge, Beck's orange is the first commercial plasticine type from which

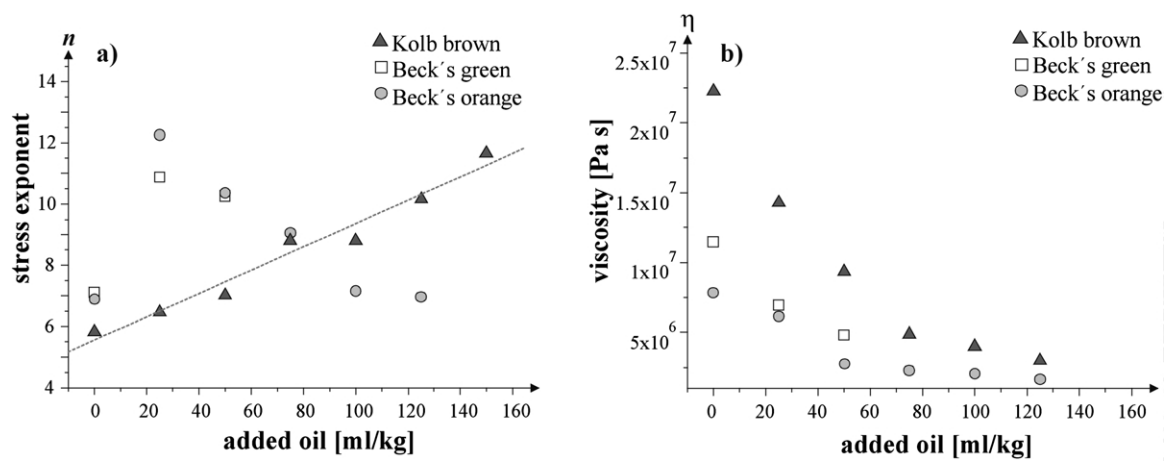

Fig. 13. Plots showing (a) stress exponent vs. amount of added oil and (b) viscosity vs. amount of added oil for the plasticine types Beck's orange, Beck's green and Kolb brown.

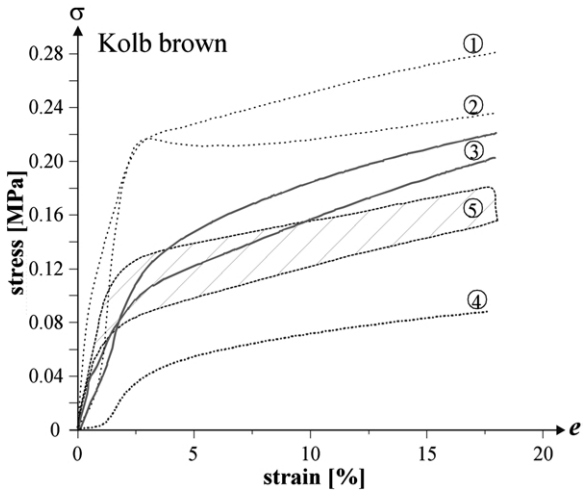

Fig. 14. Stress vs. strain diagram showing normal and abnormal flow curves for Kolb brown plasticine, measured at $\dot{E} = 1.5 \times 10^{-3}\ s^{-1}$ and $T = 25\ °C$. ① overheated sample, ② overheated sample with shear fracture, ③ prestrained sample, ④ sample including air bubbles, ⑤ flow curve interval for correct runs.

steady-state creep has been described. We suggest the particular filler to be responsible for this peculiar behaviour. Beck's orange is the only plasticine that includes potato starch, whereas the fillers of the other plasticine types consist of plate shaped like calcite, barite, kaolinite etc., which are mechanically much stronger than oil, wax and Vaseline. Thus, increasing strain might result in a shape-preferred orientation and progressive interaction of the rigid particles giving rise to strain hardening (McClay, 1976). This assumption is also supported by the higher viscosity of pre-strained plasticine (see also Dixon and Summers, 1985; Schöpfer and Zulauf, 2002).

The degree in strain hardening is further significantly controlled by the amount of fillers. Adding oil to plasticine increases the matrix/filler ratio. If this ratio reaches a critical value, the filler particles do not further interact with each other and are flowing independently in the weak organic matrix. This behaviour explains why the flow curve shows steady-state creep, if 50 and 100 ml oil are added to Beck's green and Kolb brown, respectively.

A rise in temperature also leads to a reduction in the degree of strain hardening. An increase in temperature probably decreases the length of the chains of the liquid organic phases of the plasticine matrix. Consequently the formation of entanglements that form because of the interpenetrating effect of Brownian motion (Weijermars, 1986, and references therein) is decreased, which explains the observed drop in apparent viscosity. The reason for 'warming–cooling hardening' is as yet not known.

The stress exponent of the original plasticine types shows an almost linear relation to the temperature if the latter changes within the interval considered (20–35 °C). This behaviour is an advantage for analogue modelling, as the rheological parameters for other temperatures than those considered for the present calibration can easily be determined by interpolation.

The original plasticine has a relatively high activation energy (323 ± 34–$488 \pm 22\ kJ\ mol^{-1}$). Power-law creep is a thermally activated process, and the activation energy is a measure of the energy barrier that inhibits creep. The activation energy determined for plasticine lies between the values determined for bouncing putties (Rhodorsil Gomme and Down Corning (CD3179) values at 42 ± 2 and $83 \pm 3\ kJ\ mol^{-1}$; Hailemariam and Mulugeta, 1998) and paraffin wax (β-phase = 531–624 $kJ\ mol^{-1}$; Mancktelow, 1988; α-phase = 950 and 1100 $kJ\ mol^{-1}$; Rossetti et al., 1999).

Adding oil to plasticine results in a significant change in the rheology of the original plasticine. An interpolation of viscosity and stress exponent of oil mixed plasticine is difficult because: (1) there is a non-linear relation between the apparent viscosity and the amount of added oil, and (2) the stress exponent change unsystematically, at least for Beck's orange and Beck's green plasticine. The type of fillers cannot explain the unsystematic change in stress exponent, as these are entirely different for Beck's orange and Beck's green plasticine. Moreover, we do not know why the stress exponent of Kolb brown plasticine increases linearly with added oil. For Weible white (original) plasticine, on the other hand, it has been shown that added oil results in a drop of the stress exponent from 7 to 3.4 (Kobberger and Zulauf, 1995). One possibility to explain this discrepancy is that the stress exponent of liquid polymers increases with filler contents (Weijermars, 1986) up to a critical value. Higher amounts of fillers result in a decrease of n as has been shown for Kolb brown plasticine.

It is difficult to describe the flow behaviour of plasticine using standard rheologies such as the Maxwell or Prandtl body. If we compare the stress relaxation curves with ideal curves of relaxation tests (see Weijermars, 1997, p. 129) it is obvious that plasticine behaves in a rather complex manner, exhibiting an elasto-viscoplastic flow response (Adams et al., 1997; Aydin et al., 2000). All plasticine types, except Weible special soft, reached a steady state flow, depending on the amount of added oil and rise in temperature.

5.2. Plasticine as a rock analogue

When carrying out analogue modelling, we wish to maintain geometrical, kinematical and dynamical similarity (e.g. Hubbert, 1937; Ramberg, 1981). If the modelling is restricted to small-scale structures at low strain rates, the influence of body forces (inertial and gravity) can be neglected. Geometrical similarity requires that the model is a reduced or enlarged geometric replica of the original rock. Kinematical similarity is maintained if corresponding particles are found at corresponding places at corresponding times. Dynamic similarity implies that the non-Newtonian analogue material and natural rock are geometrically and

rheologically similar, meaning that the stress–strain curves of both must have the same shape and may differ only in the scaling of the stress axis (Cobbold, 1975; Ramberg, 1981; Weijermars and Schmeling, 1986). For power-law creep, the stress exponent of the analogue material must be similar to the stress exponent of the natural rock to be modelled.

In Fig. 15 the stress exponents of the studied plasticine types and plasticine/oil mixtures are plotted against the apparent viscosities. η/n-couples obtained by previous studies are also shown. The n-values determined for plasticine and plasticine/oil mixtures range from 3.4 to 12.3. Even lower n-values should be possible if temperatures are higher than 35 °C. Thus, plasticine and plasticine/oil mixtures can be used to model the viscous flow of different rock types in the lower crust. If climb-accommodated dislocation creep and associated steady-state flow is assumed for the natural rock, Beck's orange plasticine or plasticine/oil mixtures should be used, which flow under steady-state conditions.

Moreover, rocks undergoing strain hardening during viscous creep can also be modelled using other plasticine types. We do not agree with Grotenhuis et al. (2002) who argued that plasticine cannot be used as a rock analogue because of strain hardening. There are several examples of natural rocks or minerals that show strain hardening in experiments (e.g. Carrara Marble, Schmid et al., 1980; Yule marble, Heard and Raleigh, 1972; quartz, Gleason and Tullis, 1995; Solnhofen limestone, Schmid et al., 1977). Most of the experiments show that strain hardening occurs particularly at low temperatures and/or higher strain rates. Possible candidates for strain hardening are rocks, which are subjected to decreasing temperatures during exhumation from deep structural levels where climb-accommodated steady-state creep was possible. As the temperature decreases during uplift, recovery by dislocation climb might be inhibited leading to strain hardening. Strain hardening is further important for the geometry of folds, as has been shown by Tentler (2001).

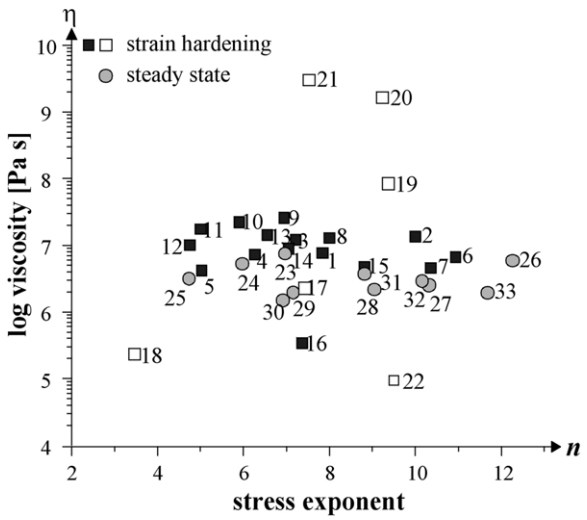

Fig. 15. Log apparent viscosity vs. log stress exponent of investigated samples (filled symbols, $T = 25$ °C, $\dot{E} = 4 \times 10^{-3}$ s^{-1}, and $e = 10\%$) and of plasticine tested in previous studies (open symbols). *Strain hardening*: (1) Beck's orange 20 °C; (2) Beck's green 20 °C; (3) Beck's green 25 °C; (4) Beck's green 30 °C; (5) Beck's green 35 °C; (6) Beck's green 25 ml oil/kg 25 °C; (7) Beck's green 50 ml oil/kg 25 °C; (8) Beck's black 25 °C (Schöpfer and Zulauf, 2002); (9) Kolb brown 20 °C; (10) Kolb brown 25 °C; (11) Kolb brown 30 °C; (12) Kolb brown 35 °C; (13) Kolb brown 25 ml oil/kg 25 °C; (14) Kolb brown 50 ml oil/kg 25 °C; (15) Kolb brown 75 ml oil/kg 25 °C; (16) Weible white special soft 25 °C; (17) and (18) Red and White plasticine $T = 20$ °C, $\dot{E} = 8 \times 10^{-3}$ s^{-1}, and $e = 5\%$ (Kobberger and Zulauf, 1995); (19)–(21) Plasticine Special Soft, Plasticine Standard Hard, and Plasticine Standard White, $T = 25$ °C, $\dot{E} = 1 \times 10^{-3}$ s^{-1}, and $e = 10\%$ (McClay, 1976); (22) White Plastilina $T = 24$ °C, $\dot{E} \approx 1 \times 10^{-3}$ s^{-1} (Weijermars, 1986); *steady-state creep*: (23) Beck's orange 25 °C; (24) Beck's orange 30 °C; (25) Beck's orange 35 °C; (26) Beck's orange 25 ml oil kg 25 °C; (27) Beck's orange 50 ml oil/kg 25 °C; (28) Beck's orange 75 ml oil/kg 25 °C; (29) Beck's orange 100 ml oil/kg 25°C; (30) Beck's orange 125 ml oil/kg 25 °C; (31) Kolb brown 100 ml oil/kg 25 °C; (32) Kolb brown 125 ml oil/kg 25 °C; (33) Kolb brown 150 ml oil/kg 25 °C.

The activation energy of plasticine is similar to that of Carrara Marble ($Q = 418$ kJ mol^{-1}; Schmid et al., 1980) and wet dunite ($Q = 420$ kJ mol^{-1}, Chopra and Paterson, 1981). Most of the other rocks (e.g. quartzite, granite, quartz diorite, diabase, anorthosite) show activation energies below 300 kJ mol^{-1} (Kirby, 1983; Ranalli and Murphy, 1987). Thus, the rock most appropriate for being modelled using plasticine is Carrara Marble because both the stress exponent and the activation energy are similar to those of plasticine (Fig. 16).

5.3. Advantages of plasticine as a rock analogue

- Plasticine is non-toxic and easily handled. Model fabrication is possible by moulding and cutting using a wire saw.
- Plasticine is not expensive and is obtainable in large quantities with different colours and strengths.
- There is no considerable volume change of plasticine with temperature.
- When changing the temperature or adding oil to plasticine, its stress exponent can be easily changed and adjusted to the stress exponents of natural rocks. It appears now to be possible to produce a model material of any n-value between 3 and 13 at various viscosities.
- Plasticine can be used to simulate deformation of rocks undergoing both steady-state creep and creep with weak to moderate strain hardening.
- In some analogue materials (e.g. paraffin wax, Manckte-low, 1988) changes in the crystal structure may take place in a temperature range below the melting point. Such allotropic transitions probably do not occur in plasticine, at least within the temperature interval considered in the present study.
- There is no problem in obtaining specimens consisting of layers of different types of plasticine, as the latter stick well together.

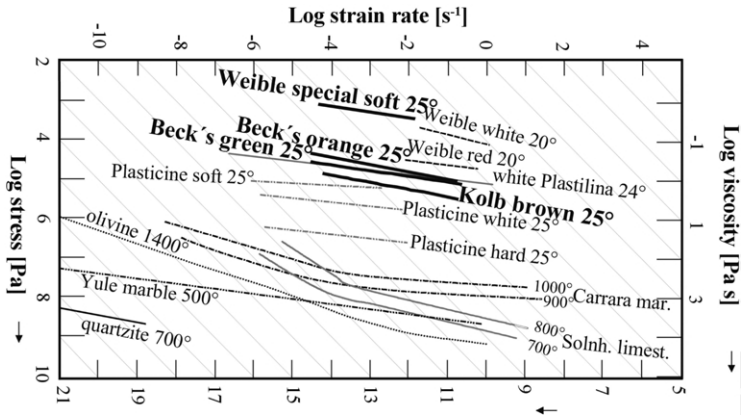

Fig. 16. Log stress vs. log strain rate diagram showing flow curves of investigated samples (at $e = 10\%$) and analogue material, tested in previous studies: Weible red and Weible white plasticine at $e = 5\%$ (Kobberger and Zulauf, 1995); Plasticine Special Soft, Plasticine Standard Hard and Plasticine Standard White at $e = 10\%$ (McClay, 1976); White Plastilina (Weijermars, 1986). Flow curves for rocks: Yule marble (Heard and Raleigh, 1972), Solnhofen limestone (Schmid et al., 1977); Carrara marble (Schmid et al., 1980); quartzite (Heard and Carter, 1968); all temperatures are in °C.

5.4. Disadvantages of plasticine as a rock analogue

- In contrast to paraffin wax and other rock analogues, plasticine is not self-lubricating. Thus, boundary effects must be reduced using oil or Vaseline to reduce friction at the contact planes between specimen and machine.
- As cooling of plasticine from high temperatures results in significant hardening, specimens cannot be obtained by pouring heated plasticine into containers with a prescribed shape.
- The microstructural flow mechanisms of crystalline rocks and plasticine are quite different. Brownian molecular motion might be important for polymeric flow (Weijermars, 1986), whereas non-linear viscous flow of rocks is attributed to dislocation motion.
- The calibration tests have shown that various consignments from one and the same supplier may differ in their rheological properties. As each new lot of plasticine has to be individually calibrated, the amount of plasticine ordered should be large enough. Similar observations have been made for paraffin wax (Mancktelow, 1988).
- The use of plasticine as a ductile (viscous) rock analogue is restricted to low strain rates ($< 10^{-3}\ s^{-1}$). Higher strain rates will cause strain localization along discrete shear planes that may result in strain softening.

Acknowledgements

We are grateful to J. Kaschta, C. Weiss and M. Heyder, Lehrstuhl für Polymerwerkstoffe, Friedrich-Alexander-Universität Erlangen-Nürnberg, for support when using the machine "Zwick/Z050" and for helpful comments. We thank E. Wosnitza for many helpful discussions and A. Weh for carrying out the X-ray diffraction analyses. We further acknowledge helpful revisions by D. Rossi and F. Storti. This study was supported by Deutsche Forschungsgemeinschaft (Zu 73/7).

References

Acocella, V., Mulugeta, G., 2002. Experiments simulating surface deformation induced by pluton emplacement. Tectonophysics 352, 275–293.

Adams, M.J., Aydin, I., Briscoe, B.J., Sinha, S.K., 1997. A finite element analysis of the squeeze flow of an elasto-viscoplastic paste material. Journal of Non-Newtonian Fluid Mechanics 71, 41–57.

Aydin, I., Biglari, F.R., Briscoe, B.J., Lawrence, C.J., Adams, M.J., 2000. Physical and numerical modelling of ram extrusion of paste materials: conical die entry case. Computational Materials Science 18, 141–155.

Brace, W.F., Kohlstedt, D.L., 1980. Limits on lithospheric stress imposed by laboratory experiments. Journal of Geophysical Research 85, 6248–6252.

Carter, N.L., Tsenn, M.C., 1987. Flow properties of continental lithosphere. Tectonophysics 136, 27–63.

Chen, W.P., Molnar, P., 1983. Focal depths of intracontinental and intraplate earthquakes and their implications for the thermal and mechanical properties of lithosphere. Journal of Geophysical Research 88, 4183–4214.

Chopra, P.N., Paterson, M.S., 1981. The experimental deformation of dunite. Tectonophysics 78, 453–473.

Cobbold, P.R., 1975. Fold propagation in single embedded layers. Tectonophysics 27, 333–351.

Cobbold, P.R., Jackson, M.P.A., 1992. Gum rosin (colophony): a suitable material for thermomechanical modeling of the lithosphere. Tectonophysics 210, 255–271.

Dixon, J.M., Summers, J.M., 1985. Recent developments in centrifuge modelling of tectonic processes: equipment, model construction techniques and rheology of model materials. Journal of Structural Geology 7, 83–102.

Gleason, G.C., Tullis, J., 1995. A flow law for dislocation creep in quartz aggregates determined with molten salt cell. Tectonophysics 247, 1–23.

Gosh, S.K., Khan, D., Sengupta, S., 1995. Interfering folds in constrictional deformation. Journal of Structural Geology 17, 1361–1373.

Grotenhuis, S.M.ten, Piazolo, S., Pakula, T., Passchier, C.W., Bons, P.D., 2002. Are polymers suitable rock analogs? Tectonophysics 350, 35–47.

Hailemariam, H., Mulugeta, G., 1998. Temperature-dependent rheologies

of bouncing putties used as rock analogs. Tectonophysics 294, 131–141.
Heard, H.C., Carter, N.L., 1968. Experimentally induced 'natural' intergranular flow in quartz and quarzite. American Journal of Science 266, 1–42.
Heard, H.C., Raleigh, C.B., 1972. Steady-state flow in marble at 500 °C to 800 °C. Geological Society of America Bulletin 83, 935–956.
Hubbert, M.K., 1937. Theory of scale models as applied to the study of geologic structures. Geological Society of America Bulletin 48, 1459–1519.
Kidan, T.W., Cosgrove, J.W., 1996. The deformation of multilayers by layer-normal compression; an experimental investigation. Journal of Structural Geology 18, 461–474.
Kirby, S.M., 1983. Rheology of the lithosphere. Reviews of Geophysics Space and Physics 21, 1458–1487.
Kobberger, G., Zulauf, G., 1995. Experimental folding and boudinage under pure constrictional conditions. Journal of Structural Geology 17, 1055–1063.
Kronenberg, A.K., Tullis, J., 1984. Flow strengths of quartz aggregates: grain size and pressure effects due to hydrolytic weakening. Journal of Geophysical Research 89, 4281–4297.
Mancktelow, N.S., 1988. The rheology of paraffin wax and its usefulness as an analogue for rocks. Bulletin of Geological Institutions of the University of Uppsala 14, 181–193.
McClay, K.R., 1976. The rheology of plasticine. Tectonophysics 33, T7–T15.
Müller, G., 1998. Starch columns; analog model of basalt columns. Journal of Geophysical Research 103, 15,239–15,253.
Murphy, D.C., 1989. Crustal paleorheology of the southeastern Canadian Cordillera and its influence on the kinematics of Jurassic convergence. Journal of Geophysical Research 94, 15,723–15,739.
Peltzer, G., Gillet, P., Tapponnier, P., 1984. Formation des failles dans un matériau modèle: la plasticine. Bulletin de la Société Géolique de France 26, 161–168.
Poirier, J.P., 1985. Creep of Crystals. High-Temperature Deformation Processes in Metals, Ceramics and Minerals, Cambridge Earth Science Series, London.
Ramberg, H., 1955. Natural and experimental boudinage and pinch-and-swell structures. Journal of Geology 63, 512–526.
Ramberg, H., 1981. Gravity, Deformation and the Earth's Crust, Academic Press, London.
Ranalli, G., 1995. Rheology of the Earth, Chapman & Hall, London, 413pp.
Ranalli, G., Murphy, D.C., 1987. Rheological stratification of the lithosphere. Tectonophysics 132, 281–295.
Rossetti, F., Ranalli, G., Faccenna, C., 1999. Rheological properties of paraffin as an analogue material for viscous crustal deformation. Journal of Structural Geology 21, 413–417.
Rossetti, F., Faccenna, C., Ranalli, G., Funiciello, R., Storti, F., 2001. Modeling of temperature-dependent strength in orogenic wedges: first results from a new thermomechanical apparatus. In: Koyi, H.A., Mancktelow, N.S. (Eds.), Tectonic Modeling: A Volume in Honor of Hans Ramberg Memoir 193. Geological Society of America, Boulder, pp. 253–260.
Schmid, S.M., Boland, J.N., Paterson, M.S., 1977. Superplastic flow in fine-grained limestone. Tectonophysics 43, 257–291.
Schmid, S.M., Paterson, M.S., Boland, J.N., 1980. High temperature flow and dynamic recrystallization in Carrara marble. Tectonophysics 65, 245–280.
Schöpfer, M.P.J., 2000. Experimentelle Untersuchung zur Bildung von Falten und Boudins. Unpublished diploma thesis, Universität Erlangen-Nürnberg.
Schöpfer, M.P.J., Zulauf, G., 2002. Strain dependent rheology and the memory of plasticine. Tectonophysics 354, 85–99.
Sofuoglu, H., Rasty, J., 2000. Flow behavior of Plasticine used in physical modeling of metal forming processes. Tribology International 33, 523–529.
Sokoutis, D., 1987. Finite strain effects in experimental mullions. Journal of Structural Geology 9, 233–242.
Talbot, C.J., 1999. Ductile shear zones as counterflow boundaries in pseudoplastic fluids. Journal of Structural Geology 21, 1535–1551.
Tentler, T., 2001. Experimental study of single layer folding in nonlinear materials. In: Koyi, H.A., Mancktelow, N.S. (Eds.), Tectonic Modeling: A Volume in Honor of Hans Ramberg Memoir 193. Geological Society of America, Boulder, pp. 89–100.
Watkinson, A.J., 1975. Multilayer folds initiated in bulk plane strain, with the axis of no change perpendicular to the layering. Tectonophysics 28, T7–T11.
Weertman, J., 1968. Dislocation climb theory of steady-state creep. Transaction of the American Society for Metals 61, 681–694.
Weijermars, R., 1986. Flow behaviour and physical chemistry of bouncing putties and related polymers in view of tectonic laboratory applications. Tectonophysics 124, 325–358.
Weijermars, R., 1997. Principles of Rock Mechanics, Alboran Science Publishing, Netherlands.
Weijermars, R., Schmeling, H., 1986. Scaling of Newtonian and non-Newtonian fluid dynamics without inertia for quantitative modeling of rock flow due to gravity (including the concept of rheological similarity). Physics of the Earth and Planetary Interiors 43, 316–330.
Wosnitza, E.M., Grujic, D., Hoffman, R., Behrmann, J.H., 2001. New apparatus for thermomechanical analogue modeling. In: Koyi, H.A., Mancktelow, N.S. (Eds.), Tectonic Modeling: A Volume in Honor of Hans Ramberg Memoir 193. Geological Society of America, Boulder, pp. 245–252.
Zulauf, G., Zulauf, J., Hastreiter, P., Tomandl, B., 2003. A deformation apparatus for three-dimensional coaxial deformation and its application to rheologically stratified analogue material. Journal of Structural Geology 25, 469–480.